Microwave synthesis of $Ti/(RuO_2)_{0.5}(IrO_2)_{0.5}$ anodes: Improved electrochemical properties and stability

Isabelle M. D. Gonzaga[a,b], Aline R. Dória[a,b], Vanessa M. Vasconcelos[a], Felipe M. Souza[c], Mauro C. dos Santos[c], Peter Hammer[d], Manuel A. Rodrigo[e], Katlin I. B. Eguiluz[a,b], Giancarlo R. Salazar-Banda[a,b*]

[a] Electrochemistry and Nanotechnology Laboratory, Institute of Technology and Research (ITP), 49032-490, Aracaju-SE, Brazil.

[b] Postgraduate Program in Process Engineering (PEP), Universidade Tiradentes, 49032-490, Aracaju-SE, Brazil

[c] LEMN – Laboratório de Eletroquímica e Materiais Nanoestruturados, CCNH – Centro de Ciências Naturais e Humanas, UFABC – Universidade Federal do ABC, CEP 09210-170, Rua Santa Adélia 166, Bairro Bangu, Santo André, SP, Brazil

[d] São Paulo State University (UNESP), Institute of Chemistry, Araraquara, Brazil

[e] Chemical Engineering Department, Faculty of Chemical Sciences and Technologies, University of Castilla-La Mancha, Enrique Costa Novella Building. Campus Universitario s/n, 13071, Ciudad Real, Spain

Corresponding author: gianrsb@gmail.com (G. R. Salazar-Banda)

ABSTRACT

The efficiency of electrochemical technology in treating water contaminated by complex organic pollutants has been widely investigated. Notwithstanding, it is still necessary to develop technologies capable of producing efficient and economically viable electrodes. In this context, the electrochemical oxidation using mixed metal oxide (MMO) anodes is a promisor alternative for wastewater treatment. However, the production of these anodes through thermal decomposition in electric furnaces demands a lot of production time. Here, we report an innovative method based on hybrid microwave irradiation to produce MMO anodes of Ti/$(RuO_2)_{0.5}(IrO_2)_{0.5}$ composition. The developed method uses simple apparatus and is faster than other conventional methods, thus decreasing the production costs. The anodes prepared at different calcination temperatures (300, 350, and 400 ºC) using microwaves irradiation were characterized by scanning electron microscopy, X-ray photoelectron spectroscopy, and X-ray diffraction, cyclic voltammetry, electrochemical impedance spectroscopy, and accelerated service life tests. Besides, the results were compared with those obtained using the conventional heating method. The microwave-produced anodes calcined at 350 ºC have the longest service lifetime, which is estimated as 15 years, which is 3.5-fold more than the conventionally-made anodes. In addition, this anode has improved electrochemical performance when compared with the conventionally-prepared anodes, showing the highest voltammetric charge (1.6-fold). Moreover, this anode removes 100% of color and 64% of TOC after 60 min of electrolysis of the model molecule methylene blue dye. Therefore, the developed method allows for producing materials with improved electrocatalytic properties and enhanced stability at short synthesis times.

Keywords: Electrocatalysis; electrochemical degradation; mixed metal oxides; Pechini.

1. Introduction

Mixed metal oxides (MMOs) anodes materials consist of inert substrates (commonly titanium) covered by a mixture of two or more metal oxides which presents improved physicochemical properties than their pure metallic equivalents [1]. RuO_2 and IrO_2 are widely studied since they combine the excellent electrocatalytic activity of RuO_2, and the high stability of IrO_2 [2]. These materials constitute an important class of solid electrocatalysts [3] that are mainly used in the chloro-alkali industry [4], in the production of oxygen and hydrogen in water electrolysis [5] and that have received attention for water and wastewater treatment [6].

Desirable characteristics considering the industrial application of these anodes are elevated surface area, high electrocatalytic activity, physical and mechanical stability, long service lifetime, and facile synthesis. Thus, the optimization of these electrodes is of great importance [7,8], existing many synthesis methods such as sol–gel method [9], decomposition of chlorides [10], and the Pechini method [11]. Commonly, the calcination step is performed in furnaces, characterized by a large temperature gradient to be established [12].

The use of hybrid microwave irradiation has become quite attractive and is used in organic synthesis [13], crystallization of nanotubes [14], the sintering of ceramics [15], among others [16]. Recently, three-dimensional carbon chemically modified electrodes were produced using hybrid microwave heating with properties enhanced [17]. Hybrid microwave heating can be performed using a susceptor material (SiC). Initially, SiC absorbs the microwaves heats up quickly, and it transfers the heat to the sample through. Volumetric heating through microwaves and the heat provided by SiC produces a more uniform temperature distribution in the volume of the sample, reducing the thermal stresses [13].

Thus, hybrid microwave heating has several advantages, such as uniform heating of the samples, accelerate diffusion mechanisms, improve the mechanical properties of a solid, increase the heating rates, minimize electrical energy expenditures, and synthesis times [18]. Hence, it is becoming a promising alternative for the synthesis of MMO anodes.

As mentioned before, the MMO presents characteristics that motivate its application in the electrochemical oxidation of wastewater containing diverse organic compounds. In particular, for effluents from the textile industry, because this is one of the most polluting industry sectors in terms of volume, color, variety (more than 100,000 commercially available types) and complexity of its released wastewater, with annual production estimated at 7×10^5 h [19]. The dyes present in these wastewaters have a complex structure, high organic load, and can be carcinogenic [20]. Azo dyes are the most commercialized among the different classes of dyes and are well-known for their high resistance to conventional treatments [21]. These wastewaters also contain large amounts of NaCl (50–80 g L^{-1}) [22] resulting from the dyeing processes for dye fixation. Thus, the electrolysis of these organic pollutants mediated by chlorides becomes very promising for the treatment of these wastewaters [23,24]. Methylene blue (MB) is a cationic dye classified as an alkaline dye, widely used in dyeing paper, wool, silk, and cotton. Besides, it is still used in tissue pigmentation (cells/tissue staining) and prescription against malaria [25]. However, excessive exposure can lead to severe serotonin toxicity, hypertension, dizziness, severe headache [25], and other illnesses [26]. Furthermore, it is necessary to develop electrodes materials less expensive to spread the application of anodic oxidation and to achieve the industrial application of electrochemical advanced oxidation processes [20].

Here we synthesized Ti/$(RuO_2)_{0.5}(IrO_2)_{0.5}$ anodes by the Pechini method using both a hybrid microwave and a conventional heating method in order to compare them. The electrodes were

physically (scanning electron microscopy, X-ray diffractometry, and X-ray photoelectron spectroscopy) and electrochemically (cyclic voltammetry, linear voltammetry, accelerated lifetime, morphology factor and electrochemical impedance spectroscopy) characterized. Moreover, the electrocatalytic efficiency of the most promising anode was evaluated towards the electrochemical degradation of the MB textile dye used here just as a model compound.

2. Experimental section

The reagents used in the pretreatment of the Ti substrate, in the synthesis of the anodes, and the electrochemical characterization were ruthenium (III) chloride hydrate ($RuCl_3$ xH_2O, 99.99%), iridium chloride ($IrCl_3$ xH_2O, 99.0%), ethylene glycol (EG) (99.8%), sulfuric acid (95.0–98.0%) and oxalic acid (99.5%) all from Sigma-Aldrich®. The anhydrous citric acid (CA) (99.5%) from Vetec®, sodium sulfate (99.0%) and hydrochloric acid (38.0%) were purchased from Neon®. Furthermore, to test the electrocatalytic efficiency of the electrodes, methylene blue (82%, Sigma-Aldrich®) and sodium chloride (99%, Neon®) were used. All solutions were prepared with ultrapure water (Gehaka MS 2000 system).

The precursor solutions were prepared according to the Pechini method [11] to produce the $Ti/(RuO_2)_{0.5}(IrO_2)_{0.5}$ anodes. First, EG was heated up to 60 ºC with the subsequent addition of CA. After the complete dissolution of CA, the metallic salts were added using an EG:CA:Metal molar ratio of 10:3:1 and then heated up to 90 °C under mechanical agitation until the total dissolution of the salts. In order to remove impurities and ensure better adhesion of the films, the titanium substrates were pre-treated in HCl (20%) for 15 min at 110 ℃, followed by 10 min in $C_2H_2O_4$ (10%) at 90 ℃, finally washing the supports with ultrapure water.

The anodes production was performed using either an electric furnace (here denoted as the conventional method - CM) and by microwave hybrid (here denoted as hybrid microwave method-MW). To produce the anodes made by conventional heating, an electric furnace EDG 3P-S muffle model 3000 was used. After painting the precursor solution over the substrate, the anodes are transferred to the furnace and treated first at 130 ºC for 30 min for solvent evaporation, then at 250 ºC for 10 min for layer adherence and finally the calcination at 300 ºC, 350 ºC or 400 ºC at a heating rate of 5 ºC min^{-1} to eliminate any remaining organics. This procedure was repeated four times until the deposited mass attains a value of 1.2 mg cm^{-2} [27]. For the microwave heating, a domestic microwave from Consul (700w and 2.45 GHz) was used. In order to perform the hybrid heating (Fig. 1) and to achieve homogeneous surfaces, a box of insulating bricks was used and, inside it, SiC plates (suppressors) that present high dielectric constant (ε_r = 9.7) was employed [18].

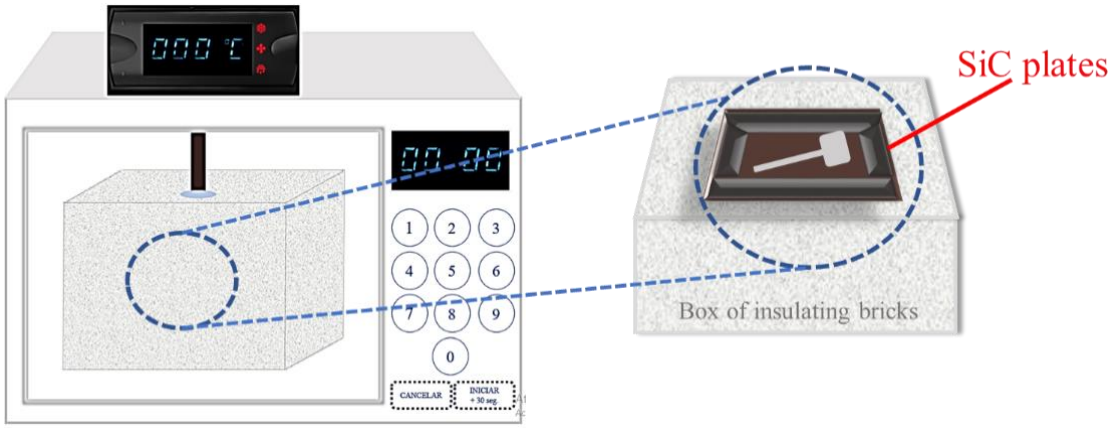

Fig. 1: Scheme of hybrid heating apparatus with microwave irradiation.

The electrodes are inclined at 45 degrees during thermal treatment, and the irradiation was applied for 18, 23, and 28 min to achieve 300, 350, and 400 ºC, respectively. Comparably to

conventional heating, the heating procedure was repeated four times until the electrodes reached a mass of around 1.2 mg cm^{-2}.

The diffraction patterns were obtained in a Brucker D8 Advance diffractometer using irradiation Cu K_α (λ = 0.15406 nm) in the range of $20^o < 2\theta < 80^o$, with a scan rate of 0.02^o min^{-1}. Scanning electron microscopy (SEM) analyses were performed using a JEOL JCM 5700 microscope at a 10 kV voltage with 500× and 2000× magnification. X-ray photoelectron spectroscopy (XPS) measurements were carried out by a Thermo Scientific K-Alpha$^+$, spectrometer a monochromated with Al Kα X-ray source radiation (hν = 1486.6 eV) and a spot diameter of 400 μm at base pressure below of 5×10^{-7} Pa. Binding energies the spectra were referenced against the C 1s component of adventitious carbon at 284.6 eV. Peak energies were given with an accuracy of 0.1 eV. The spectra were deconvoluted using a Levenberg–Marquardt algorithm of the CasaXPS software.

The electrochemical measurements were performed in a potentiostat/galvanostat (Autolab, model PGSTAT30), with a single compartment electrochemical cell composed of three electrodes: platinum counter electrode, Ag/AgCl reference electrode (KCl, 3 mol L^{-1}) and the produced $Ti/(RuO_2)_{0.5}(IrO_2)_{0.5}$ anodes as a working electrode. All electrochemical characterizations were carried out in 0.5 mol L^{-1} H_2SO_4 solutions. Cyclic voltammetry measurements were carried out in a potential range from 0.2 to 1.2 V vs. Ag/AgCl at a scan rate of 40 mV s^{-1}. The voltammetric charge was obtained after the integration of the cyclic voltammetry curves, and the result multiplied by the inverse of the scan rate. According to the methodology proposed by Da Silva et al. [28], the morphology factor and capacitance were calculated by cyclic voltammetry at different scan rates (10–300 mV s^{-1}).

Electrochemical impedance spectroscopy (EIS) experiments were performed covering the frequency range 0.01 Hz – 10 kHz with a logarithmic distribution of 10 frequencies per decade using

a sine signal amplitude of 5 mV. The potential applied in the EIS measurements was the potential regions of onset of the oxygen evolution reaction observed for each electrode (1.1V vs. Ag/AgCl). Accelerated service life tests were performed in 1.0 mol L^{-1} H_2SO_4 solution with an applied current density of 1.0 A cm^{-2}. The anodes were considered deactivated when the measured potential reached 10 V. Wang et al. [29] have developed a relationship between anode service life (S_L) and current density (i) can be represented by Eq. 1.

$$S_L = S_{La}(i_a/i_e)^n \quad (1)$$

Where, S_{La} is an accelerated service life, i_a is the accelerated current (1 A cm^2), i_e is the current during electrolysis (0.30 A cm^2), and n is a coefficient and varies according to the electrolyte used (H_2SO_4 = 1.3).

The oxidation of MB dye was carried out in a 220 mL electrochemical glass cell under stirring at 1000 rpm, controlled and monitored by a DC Power Supply PS 5000 ICEL for the potential application, using a platinum counter electrode. At pre-determined time intervals, samples were collected, and 20 µL of a $NaHSO_3$ solution (0.5 mol L^{-1}) was added immediately to quench the residual oxidants. The degradation efficiency was evaluated by modifying different parameters. Initially varying the electrolyte in 0.1 mol L^{-1} Na_2SO_4 with addition of 0, 10, 20, and 30 mmol L^{-1} NaCl, applied potential of 5, 10, and 15 V (i = 6, 25, and 54 mA cm^{-2}) and pH 2, 6 and 10. MB absorption spectra were obtained by using a UV-Vis Hach DR 5000 spectrophotometer for analysis of compound concentration and discoloration during treatment. MB concentration was monitored using a calibration curve determined at 664 nm. The discoloration was analyzed from the curve

integration value obtained by a spectral scan in the range from 400 to 800 nm. The percentage of color removal was calculated by using Eq. 2.

$$Color\ removal\ (\%) = \frac{A_0 - A_t}{A_0}\ x\ 100 \quad (2)$$

Where, A_0 and A_t there are the absorbance initial and final at the initial time and the time t, respectively.

The removal of total organic carbon (TOC) content was calculated using Eq. 3, where TOC_0 and TOC_t are the TOC values at the initial time and time t, respectively. The analyses were performed on a Shimadzu TOC analyzer, model TOC-L.

$$TOC\ removal\ (\%) = \frac{TOC_0 - TOC_t}{TOC_0}\ x\ 100 \quad (3)$$

Energy consumption (EC) was calculated as a function of TOC removal, as shown in Eq. 4, where E is the applied potential (V), I is the applied current (A), Δt is the electrolysis time (h), and V is the volume (L).

$$EC\ = \frac{EI\Delta t}{V(TOC_0 - TOC_t)} \quad (4)$$

Mineralization current efficiency (MCE) was calculated using Eq. 5 [30]. Where F is the Faraday's constant (96.485 C mol^{-1}), and Δt is the electrolysis time in s.

$$\text{MCE} = \left[\frac{(TOC_0 - TOC_t)2.87}{8I\Delta t}\right] . FV \quad (5)$$

3. Results and discussion

3.1. Physical characterization

Figure 2 shows the SEM images of the electrodes Ti/$(RuO_2)_{0.5}(IrO_2)_{0.5}$ prepared by conventional (CM) (Fig. 2b, 2d, and 2f) and microwave (MW) (Fig. 2a, 2c, and 2e) heating. The films prepared by both methods display a typical "cracked-mud" morphology, which results from the different expansion rates between the titanium substrate and the metal oxide film during the calcination process [7,31]. On the other hand, probably due to the rapid heating of the microwaves, the films obtained are more homogeneous than anodes produced conventionally.

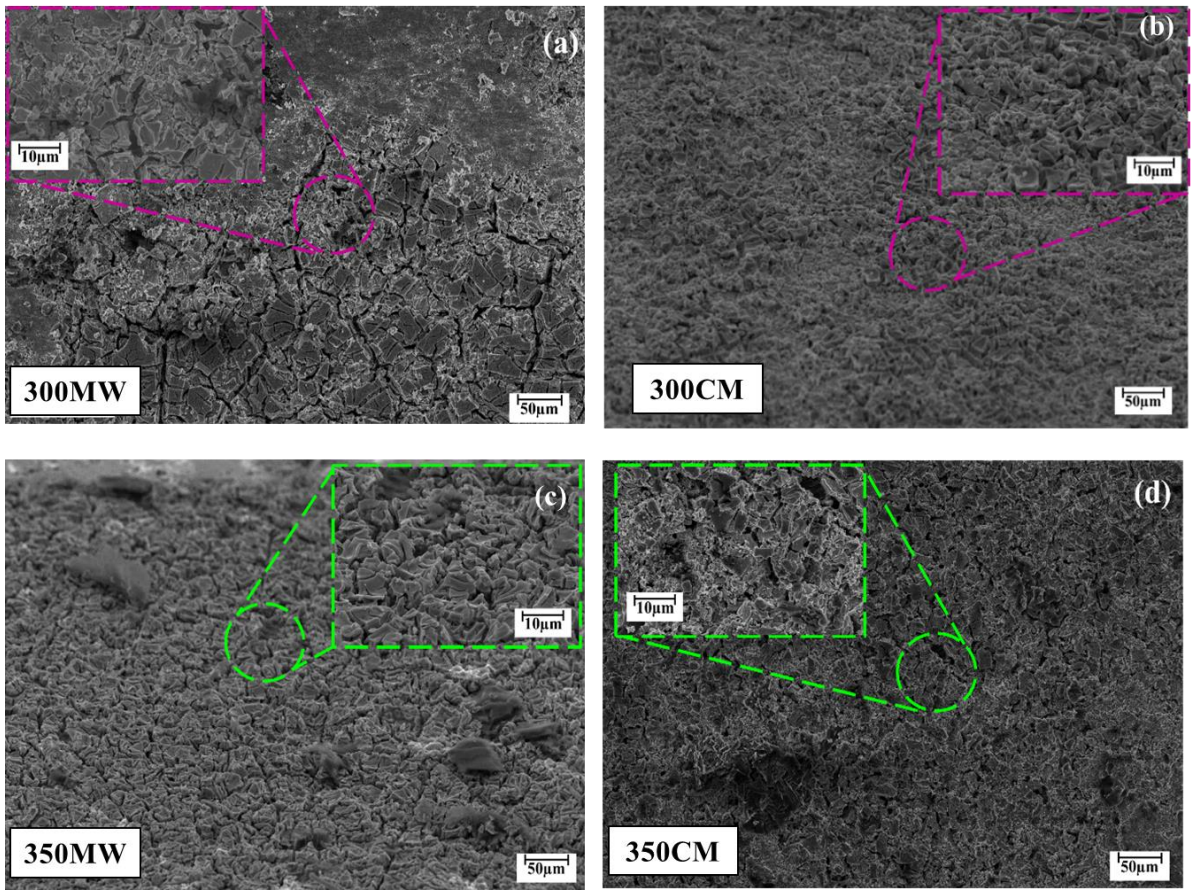

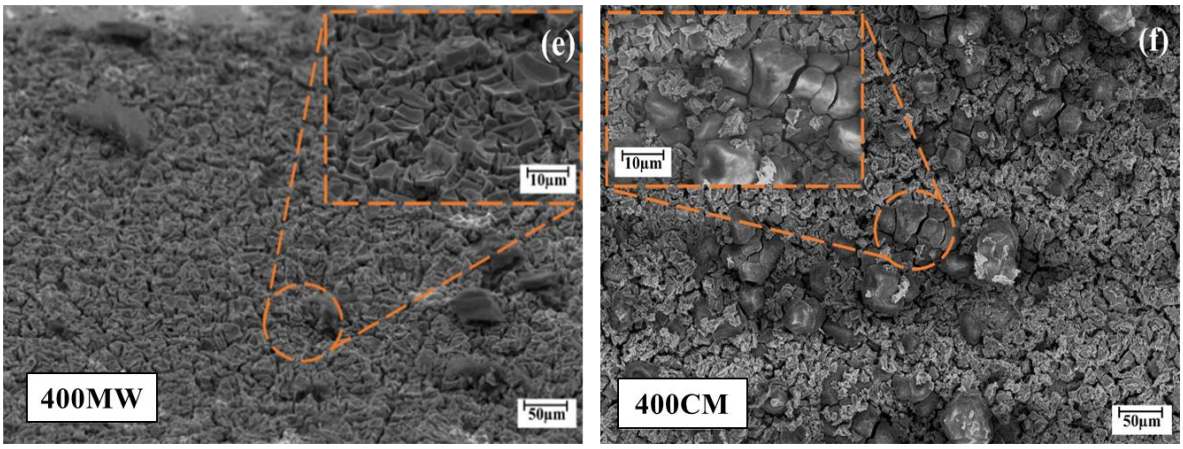

Fig. 2: SEM images of Ti/$(RuO_2)_{0.5}(IrO_2)_{0.5}$ anodes made by microwave heating at (a) 300 ºC (c) 350 ºC and (e) 400 ºC and by conventional heating at (b) 300 ºC, (d) 350 ºC and (f) 400 ºC. SEM images with a magnification of 500× (inset with a magnification of 2,000×).

The X-ray diffraction (XRD) patterns (Fig. 3) show, according to the Joint Committee on Powder Diffraction Standards (JCPDS), ruthenium oxide (JCPDS 40-1290) and iridium oxide (JCPDS 15-087) peaks. The most prominent peaks are from the metallic Ti of the substrate. Ruthenium and iridium present similar cationic radius (0.620 and 0.625 Å, respectively) and their oxides have the rutile-type crystal structure with peaks corresponding (110), (101), (211) and (002) relative to the angles at 28, 34.7, 52 and 54 degrees, respectively [1]. Therefore, mixed RuO_2–IrO_2 phases are easily formed [32], as found in this work.

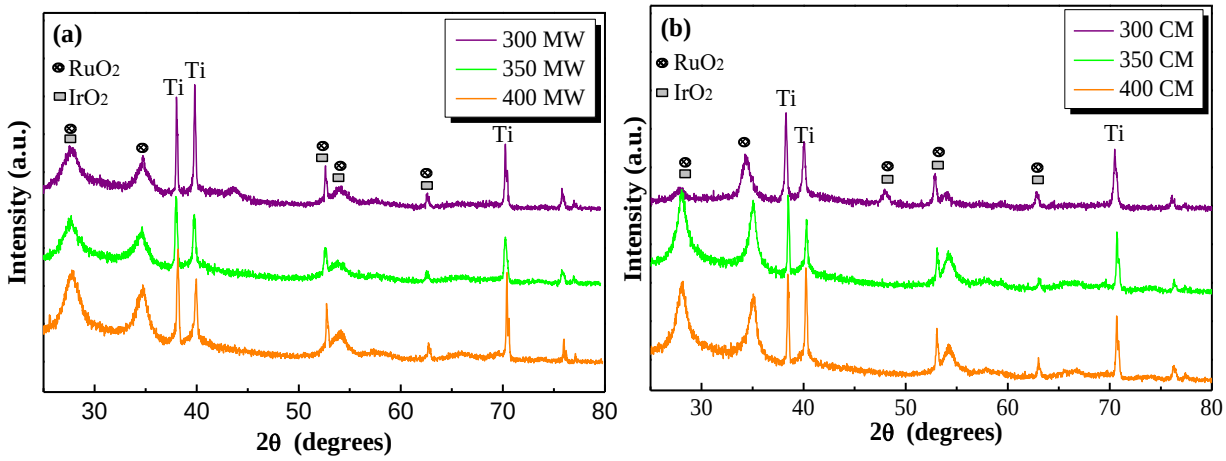

Fig. 3: XRD patterns of Ti/$(RuO_2)_{0.5}(IrO_2)_{0.5}$ anodes synthesized using (a) microwave and (b) conventional heating.

The electrodes prepared by conventional heating have more defined peaks than the microwave-made anodes, which may suggest a higher degree of crystallinity. In order to confirm this, crystallite sizes were calculated according to the Scherrer formula. Values were found to be lower for the microwave prepared anodes (7.3, 7.3, and 8.9 nm for 300, 350, and 400 ºC) when compared with those obtained for furnace prepared (12.0, 11.2, and 9.3 nm for 300, 350 and 400 ºC). Rapid heating and cooling may justify such behavior during microwave heating that may hinder oxide crystallization [32]. The XRD results revealed that both methods ensure the formation of desired oxides.

XPS analyses were performed to explore the oxidation state and surface composition of samples treated at 350 ºC. XPS survey scans identified Ru, Ir, Ti, C, and O, for both electrodes calcined at by conventional and microwave methods (Fig. S1 and S2 (without Ti)). The survey spectra of the coating made by the conventional method show a lower intensity of the Ru and Ir peaks compared to the spectra of the microwave-made anode.

The atomic ratios between Ru and Ir are close to the expected nominal value of 50:50. However, the coating prepared by the microwave method contained a higher amount of oxygen and a lower amount of C (Table 1). The concentration level of carbon of the microwave sample is in the range usually observed in an *ex-situ* analysis for surface contamination by adventitious carbon. These data suggest that for the anodes calcined at 350 ºC, the microwave method is more appropriate to eliminate the carbon from the precursor solutions during the coating preparation.

Table 1: Elemental composition obtained by XPS for the developed samples treated at 350 °C.

Method	**Coating**	**Atomic concentration (%)**
Microwave	Ru	18.8 ± 0.6
	Ir	19.2 ± 0.5
	C	17.7 ± 1.6
	O	44.3 ± 0.9
Conventional	Ru	12.0 ± 0.5
	Ir	10.0 ± 0.4
	C	43.9 ± 2.1
	O	34.1 ± 1.3

The deconvoluted high-resolution Ru 3d spin-orbit spitted spectra (Fig. 4) (Ru $3d_{5/2}$ and Ru $3d_{3/2}$) revealed for both electrodes the presence of Ru^{4+}, RuO^{6+} and RuO^{8+} oxidation states centered at 280.8 eV, 281.9 eV, 283.4 eV, and 286.7 eV [33-36], which overlap with the C 1s spectrum of residual carbon (Fig. 4a and 4b) [37]. The presence of a higher concentration of carbon affects primarily the conventionally prepared anode with components assigned to hydrocarbon, alkoxy, and

carboxyl groups at 284.7 eV, 286.4 eV, 288.8 eV, respectively [38]. The fitted Ir 4f spin-orbit spectra show the presence of the predominant metallic phase but also the Ir^{4+} oxidation state and a satellite peak (Fig. 4c and 4d) [39]. The predominance of iridium on the electrode surface can directly influence its service lifetime. It is important to note that Ti was found only in the electrode produced by the conventional method, confirming that the MW produces improved recovering of the substrate. The main modifications of the bonding environment that can be observed are the higher intensities of the Ru^{2+} and the Ir^0 sub-peaks and lower carbon content of the sample prepared by the microwave method, suggesting a distinct electrochemical activity of this electrode compared to that conventionally treated.

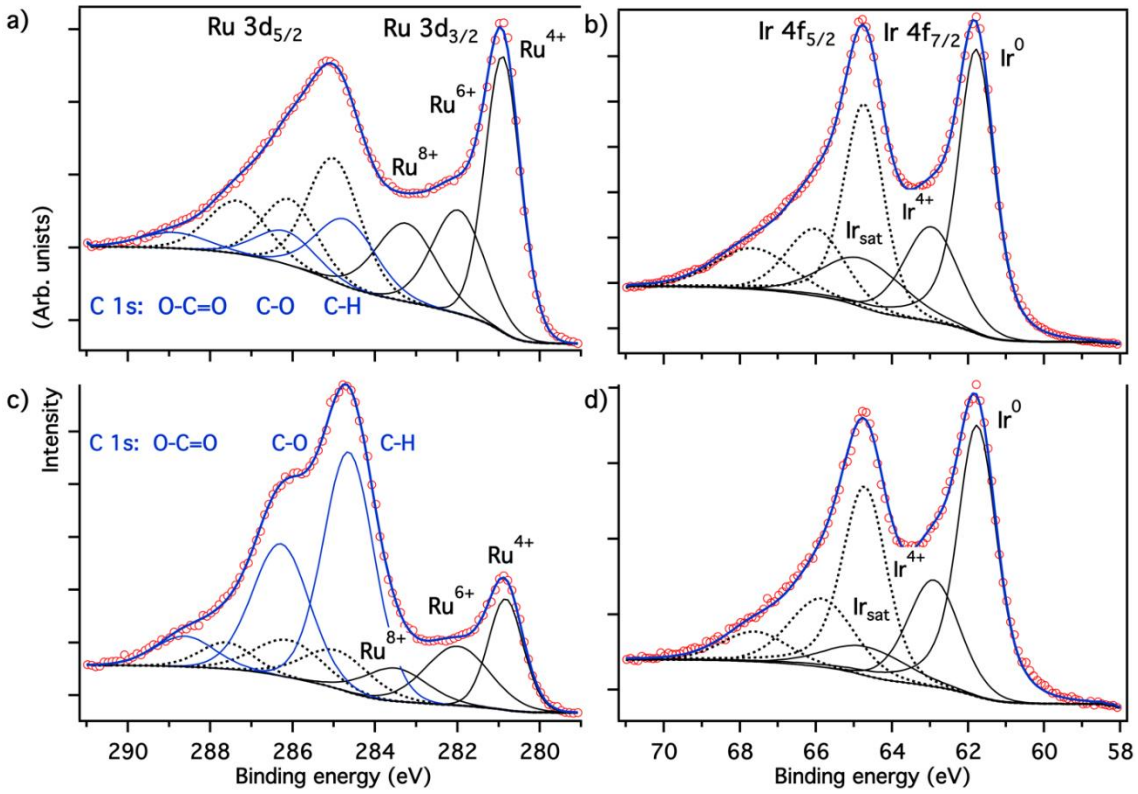

Fig. 4: Deconvoluted Ru 3d high-resolution spectra of Ti/$(RuO_2)_{0.5}(IrO_2)_{0.5}$ anodes synthesized at 350 °C using a) microwave and c) conventional heat treatment, and fitted Ir 4f high-resolution spectra for Ti/$(RuO_2)_{0.5}(IrO_2)_{0.5}$ anodes synthesized using b) microwave and d) conventional

method.

3.2. Electrochemical Characterization

Cyclic voltammetry profiles were obtained for the anodes prepared within a potential range of 0.2–1.2 V *versus* Ag/AgCl (Fig. 5). For electrodes synthesized at 300 °C, two oxidation state changes are few visible at 0.4, and 1.0 V *versus* Ag/AgCl which can be attributed to the Ru (III)/Ru (IV) and Ir (III)/Ir (IV) transition (represented in Fig. 5a), as reported by Mattos-Costa et al. [1]. According to the literature [35-40], the voltammograms of pure Ru or Ir electrodes are well defined, clearly showing the anode and cathode peaks related to the redox pairs. However, in MMOs, these peaks are not very pronounced when compared to the voltammograms of their respective pure oxides. Because of this, in the voltammograms recorded for the anodes calcinated at 350 and 400 ºC, the anodic and cathodic peaks are not observed. Such behavior may have occurred due to the displacement of the peaks by the formation of the valence bond between the Ir and Ru oxides [41].

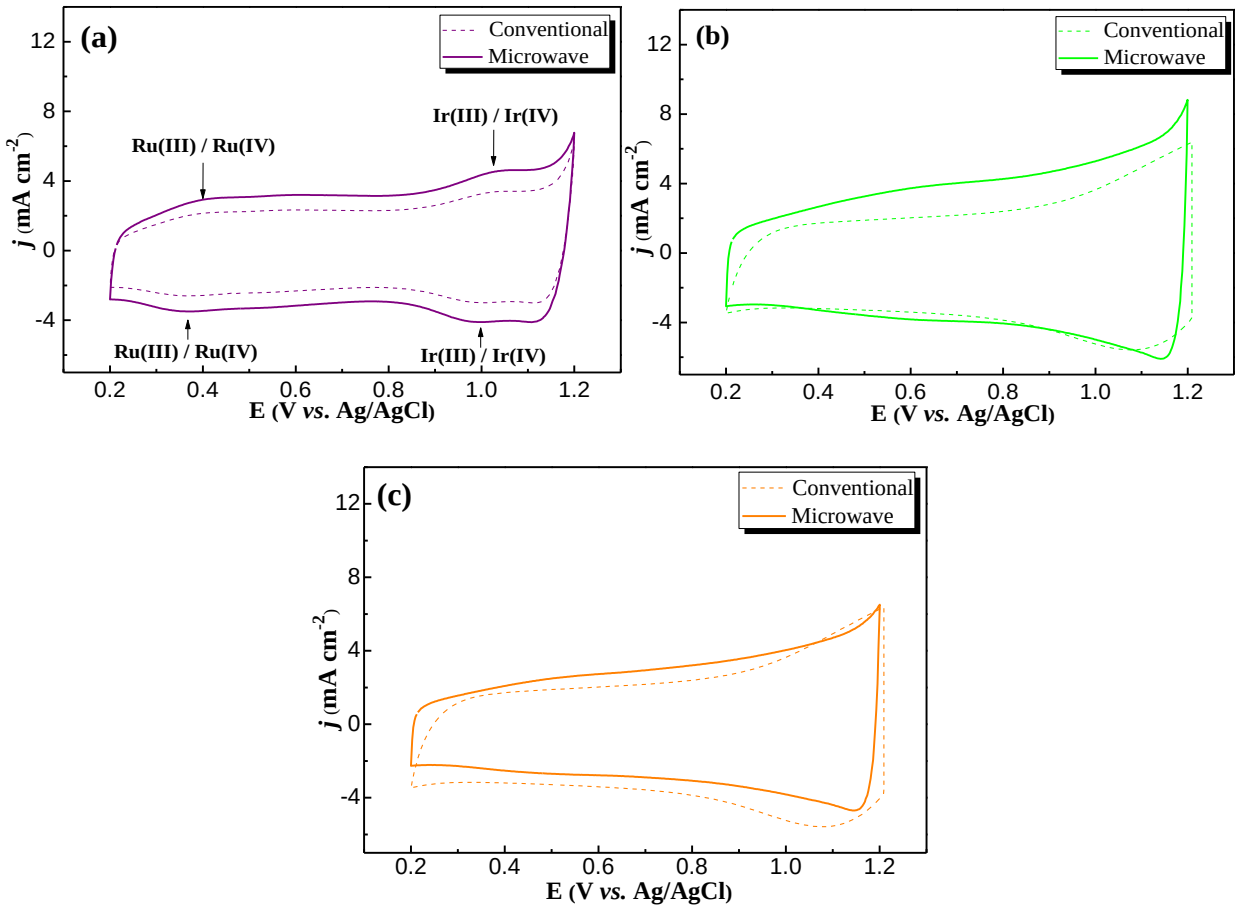

Fig. 5: Cyclic voltammograms recorded at 40 mV s^{-1} for the Ti/$(RuO_2)_{0.5}(IrO_2)_{0.5}$ anodes prepared using conventional and microwave heating at temperatures of (a) 300 (b) 350 and (c) 400 °C in 0.5 mol L^{-1} H_2SO_4 electrolyte.

The electrocatalytic activity of MMO anodes depends fundamentally on the number of active sites accessible to the electrolyte. Thus, the total voltammetric charge density (q*) can be considered as a relative measure of the electrochemically active area or the number of active sites in the electrocatalytic layer of the MMOs [31]. Therefore, the higher the q* values, the greater is the electrocatalytic activity. In this sense, the anodes made by MW display the highest values q* for all temperatures (Table 2). The q* values obtained for the Ti/$(RuO_2)_{0.5}(IrO_2)_{0.5}$ anodes made by

microwave heating at 300, 350, and 400 ºC are 1.4, 1.5, and 1.3 times higher than CM anodes at their respective temperatures.

Dória and coworkers [27] synthesized Ti/RuO_2 electrodes with different layer thicknesses (8.2, 13.7, and 16.5 μm) and compared them with a commercial DSA. Characterizations performed in acid media showed the voltammetric profile characteristic of ruthenium-based electrodes. As the number of layers (8, 14, and 20) increased, the voltammetric charge decreased (17.8, 12.6, and 8.8 mC, respectively) and the size of the crystallite (27.1, 27.1, and 39.5nm) increased. These outcomes were directly related to longer heat treatment time. As a consequence, and due to the rapid time of thermal treatment, the anodes synthesized here by microwaves obtained small crystallite size, which results in higher voltammetric charges.

Santos et al. [32] synthesized Ti/$(RuO_2)_{0.5}(IrO_2)_{0.5}$ anodes by using CO_2 laser and conventional heating methods. The laser-prepared anode displayed a crystallite size 3.9 times smaller and a voltammetric charge 1.7 times larger than the conventionally-prepared anode. Such behavior was directly related to the rapid thermal treatment (about 15 min per layer). In this context, it has been reported that low crystalline oxides have higher values of voltammetric charge, thus corroborating the results obtained in this work.

According to Audichon et al. [42], voltammetric current density values of MMOs increase commonly when crystallite/particle size is smaller, because of increasing active sites favoring charge-storage at the surface of the anodes. The results observed in the present study are well-correlated with the previously observed from XRD results.

Moreover, regarding the active sites present at the anode surface, Audichon et al. [43] have shown that reactions occur at all active sites when low scan rates are used because the electrolyte can diffuse throughout the electrocatalytic layer. Thus, at high scan rates, reactions take place only

at the most accessible active sites. Consequently, the morphology factor (φ) is related to the regions of the layer that are most difficult to access, and the influence of the porosity of the film can be determined according to Eq. 6 [28].

$$\varphi = \frac{Cd,i}{Cd} \quad (6)$$

Where $C_{d,i}$ and C_d represent the internal and the total surface capacitance of the film, respectively. The value of φ can range from 0 to 1, with values close to 0 indicating that the internal sites of the electrode have a small influence on total differential capacitance, and values close to 1 indicate that the electrode has a large internal area.

Table 2 shows that in all cases, higher values of φ are obtained for conventionally made anodes when compared with the microwave made anodes. Thus, it can be stated that conventional heating yield surfaces with higher porosity, or still deeper cracks than microwave heating. However, when analyzing the number of active sites, an enormous amount of external active sites for microwave-made anodes can be observed, which can be attributed to higher film roughness [32, 44, 45]. Thus, corroborating the SEM data (Fig. 2), where microwave heating produced rough surfaces.

Table 2: Effect of the temperature and the synthesis method of the developed MMO anodes on the total voltammetric load (q *), total differential capacitance (C_d), external ($C_{d,e}$), and internal ($C_{d,i}$), and morphology factor (φ).

Anode	***q**** (mC cm^{-2})	C_d (mF cm^{-2})	$C_{d,e}$ (mF cm^{-2})	$C_{d,i}$ (mF cm^{-2})	φ ($C_{d,i}$ /C_d)

300 conventional	87.28	47.05	2.19	44.86	0.95
350 conventional	99.47	59.4	7.49	51.91	0.87
400 conventional	86.25	37.6	5.49	32.11	0.85
300 microwave	119.92	73.37	17.58	55.79	0.76
350 microwave	143.50	74.96	23.70	51.26	0.69
400 microwave	108.85	55.43	41.72	17.10	0.24

Figure S3 shows the dependence of the voltammetric capacitive current density, j_c, with the scan rate, ν, for the Ti/$(RuO_2)_{0.5}(IrO_2)_{0.5}$ anodes. Two linear segments are observed in the domains of high and low scan rates, respectively. Such behavior is similar to that observed in the literature for highly rough films [8,43,46]. Additionally, at low scan rates, the current densities for the conventionally and microwave made anodes are similar, but at higher scan rates, the current densities for microwave made anodes are much higher. Therefore, the external capacitance values are higher, thus influencing the morphology factor more than the internal capacitance, corroborating data in Table 2.

EIS measurements were performed for all the developed anodes (Fig. 6). All spectra exhibit poorly developed semicircles in the Nyquist diagrams. Such behavior is associated with roughed surfaces, characteristics of thermally synthesized oxide films [32,47]. Additionally, it is known that the arc size corresponding to the charge transfer resistance, where the smallest arc indicates a higher charge transfer on the electrode surface [37].

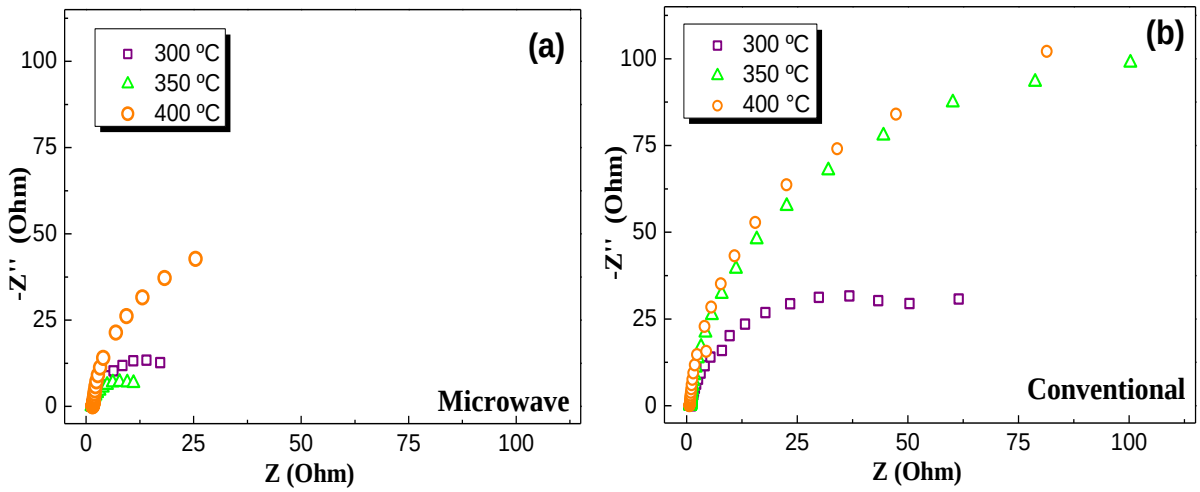

Fig. 6: Nyquist diagrams of Ti/$(RuO_2)_{0.5}(IrO_2)_{0.5}$ electrodes taken in 0.5 mol L^{-1} H_2SO_4 solutions at 25 °C. Anodes prepared by using (a) microwave and (b) conventional heating

Microwave-made electrodes, regardless of the calcination temperature, have smaller arcs (Fig. 6a) than the conventionally-made anodes (Fig. 6b), which is related to improved charge transfer on the surfaces of these electrodes [49,50]. Moreover, considering the calcination temperature, the use of the intermediate temperature during microwave heating produces electrodes with the lowest resistance to charge transfer. Instead, for anodes made by using conventional heating, the use of the lowest studied temperature leads to low charge transfer resistances.

Accelerated service life tests were performed in order to analyze the stability of the MMO anodes. A current density of 1.0 A cm^{-2} was applied to perform these analyses with the conventional and microwave-made anodes in 1.0 mol L^{-1} H_2SO_4 solution (Fig. 7). The MMO anodes are considered deactivated when a rapid increase in potential occurs, reaching 10 V [10].

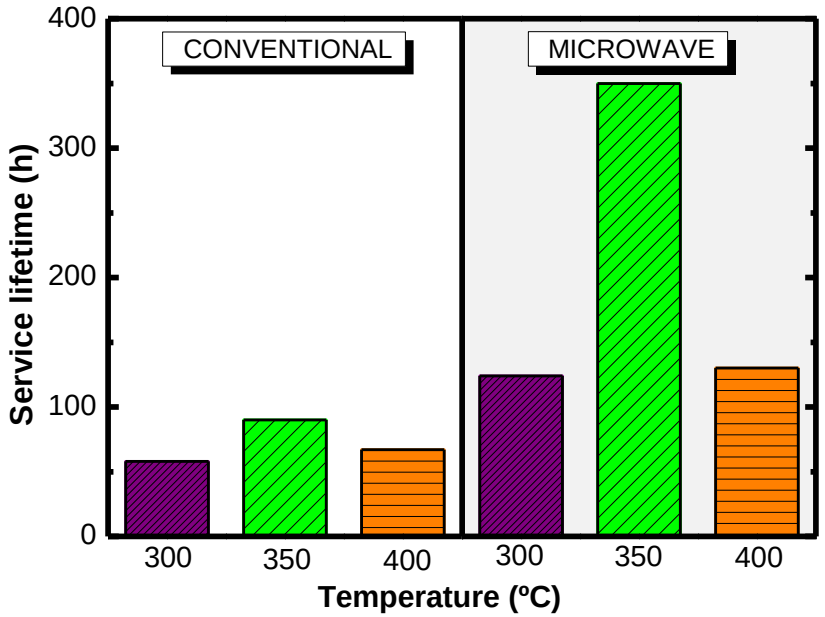

Fig. 7: Accelerated service life tests made for the Ti/$(RuO_2)_{0.5}(IrO_2)_{0.5}$ anodes obtained after conventional and microwave calcination in 1.0 mol L^{-1} H_2SO_4 electrolyte at 1.0 A cm^{-2}.

Microwave heating drastically increased the lifetime of the anodes, which were 2.1, 3.8, and 1.9 times longer for anodes calcined at 300, 350, and 400 ºC, respectively than the conventionally prepared ones. The longer service life observed for the microwave-synthesized anodes can be attributed to the more homogeneous previously seen in SEM images (Fig. 2). As a result, the presence of multiple cracks on the conventional anode surfaces facilitates the penetration of the electrolyte solution through these cracks and accelerates film corrosion [32].

Santos et al. [32] synthesized Ti/$(RuO_2)_{0.5}(IrO_2)_{0.5}$ composition anodes using a CO_2 laser and by conventional heating. The use of CO_2 laser (as well as the use of microwave, the method used in this work), produced anodes with surfaces that are more compact and with longer lifetime (1.6 times), compared to the conventional Pechini method. Additionally, by using the equation proposed by Wang et al. [29], we can estimate the service lifetime. For the 350ºC microwave-synthesized

electrode, the lifetime is about 15 years. It is showing a considerable duration when compared to existing studies in the literature (8 and 12 years) [35,47].

The challenge in environmental electrochemistry is to produce highly electrocatalytic, cheap, and mainly durable anodes. Notably, the hybrid heating using microwaves improved the electrochemical characteristics of the electrodes, especially the lifetime. Since the electrode made by hybrid heating using microwaves at 350 °C displayed the most extended service life and the best physicochemical characteristics. Thus, this electrode was chosen to prove the efficiency of the anodes made here in degrading the methylene blue dye just used here as a model of pollutant.

3.3. Electrocatalytic efficiency towards the degradation of the model pollutant

The efficiency in the electrochemical degradation of organic compounds using MMO anodes depends on several parameters such as anode composition, electrolyte, pH, temperature, potential, and applied current. Thus, we studied the influence of pH, NaCl concentration, and the potential applied to the degradation of MB using the anode with the best physicochemical characteristics (i.e., 350 ºC - microwave heating) (Fig. 8).

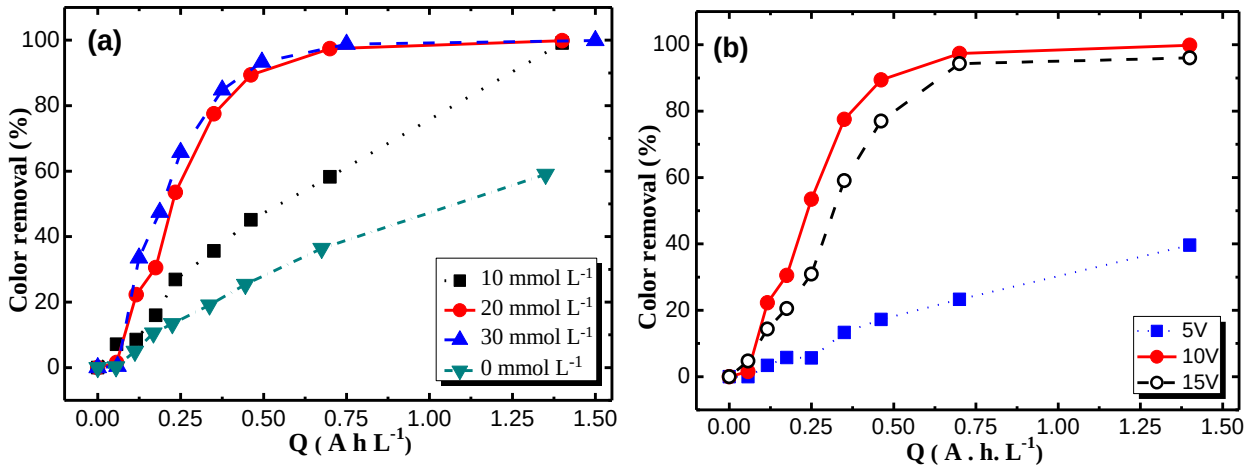

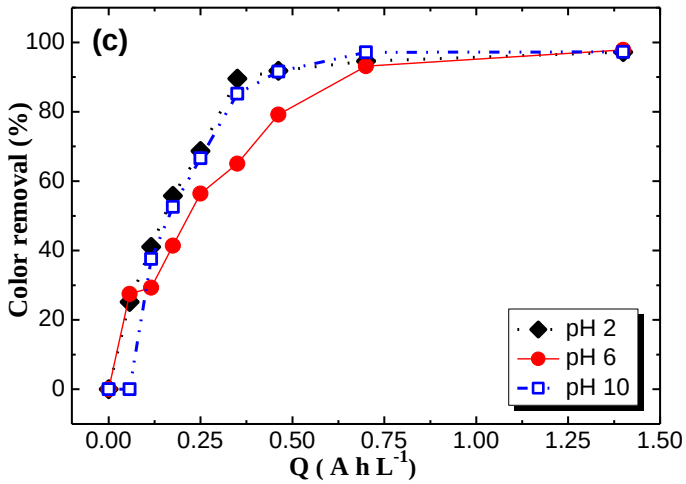

Fig. 8: (a) Effect of NaCl concentration on color removal of solutions MB dye, using (▼) 0.1 mol L^{-1} Na_2SO_4, (■) 0.1 mol L^{-1} Na_2SO_4 + 10 mmol L^{-1} NaCl, (●) 0.1 mol L^{-1} Na_2SO_4 + 20 mmol L^{-1} NaCl and (▲) 0.1 mol L^{-1} Na_2SO_4 + 30 mmol L^{-1} NaCl in 10 V and pH 6. (b) Effect of the voltage applied on color removal being (■) 5 V, (●) 10 V and (○) 15 V in 0.1 mol L^{-1} Na_2SO_4 + 20 mmol L^{-1} NaCl media at pH 6 and (c) Effect of pH on color removal, being (♦) pH 2, (●) pH 6 and (□) pH 10 V, and applying 10 V and 0.1 mol L^{-1} Na_2SO_4 + 20 mmol L^{-1} NaCl electrolyte in MB_o 50 mg L^{-1}.

The electrolyte used is a very relevant parameter in the electrochemical removal of organic compounds. Fig. 8a shows the discoloration, without and with NaCl (0, 10, 20, and 30 mmol L^{-1}) added to the 0.1 mol L^{-1} Na_2SO_4 solution as a function of the charge applied. In the absence of NaCl, only 59.0% of the color was removed, whereas, in the presence of NaCl, all conditions showed complete color removal after one hour of electrolysis. Likewise, increasing NaCl concentration increases the rate of dye discoloration, while the removal of TOC (Table 3) was slightly higher for the 20 mmol L^{-1} NaCl solution (see Fig. S4). This fact can be attributed to oxidation by active chlorine species since electrolyzes in the presence of Cl^- ions lead to in-situ chlorine (Cl_2)

production, and the formation of dissolved active chlorine species, leading to oxidation of the dye within the solution. The higher the chloride concentration, the higher is the generation of active chlorine species, leading to the increasing degradation efficiency of the organic compounds; however, a large number of active chlorine species also can lead to the formation of intermediate compounds even more resistant to electrochemical oxidation [50]. Therefore, it is vital to study and optimization of the NaCl concentration.

Without NaCl, oxidation of MB occurs predominantly at the electrode surface, through the chemisorbed oxidizing species generated by water oxidation, which means the process depends on mass transport, limiting the oxidation of the dye. Nevertheless, these oxides have a lower oxidation capacity than physisorbed hydroxyl radicals [51, 52]. Therefore, neither the complete discoloration nor the TOC removal is attained in the absence of chlorides.

Increased TOC removal occurs with increasing NaCl concentration until 20 mmol L^{-1}. Despite the high efficiency in color removal in the presence of chlorides, recalcitrant organochlorine compounds can be generated by oxidation. A similar result was found by Panizza et al. [53] during MB removal, which increased the NaCl concentration increased the removal of TOC. Therefore, here, this condition led to lower energy consumption (609.8 kWh kg^{-1}) and higher mineralization current efficiency (15.0%) (Table 3). Consequently, the optimum condition for electrolyte concentration was 20 mmol L^{-1} NaCl.

Table 3: Effect of variables: NaCl concentration (C_0NaCl), applied voltage (E), and pH on energy consumption and current efficiency in the process of electrochemical oxidation of MB.

Variables		**TOC removal (%)**	**EC (kWh kg^{-1})**	**MCE (%)**
C_0NaCl	10.0	56.0	930.3	9.6

(mmol L^{-1})	20.0	64.0	609.8	15.0
	30.0	60.0	842.1	11.0
E (V)	5.0	35.0	139.4	32.1
	10.0	64.0	718.0	12.0
	15.0	55.0	2426.3	5.5
pH	2.0	33.0	2869.2	3.1
	6.0	64.0	808.0	11.0
	10.0	20.0	966.1	9.2

Note that despite complete color removal, the maximum TOC removal was 64.0% (20 mmol L^{-1} de NaCl). This behavior shows that it is simpler to remove color by cleavage of chromophore groups, which results in discolored intermediates in the solution [53]. For this reason, discoloration occurs faster compared to the removal of the organic charge since the oxidation of aromatic rings takes relatively longer times. Besides, for TOC removal, organic carbon must be converted into carbon dioxide [54].

Similar behavior was found by Liu et al. [55], where the TOC removal profile showed exponential behavior. In the first 90 min, rapid COD removal was observed, later TOC removal was slow. These authors concluded that the breakdown of aromatic groups into aliphatic compounds is slow. Thus, achieving full-color removal was possible, but achieving complete mineralization was not. Another determining factor of the efficiency of the electrochemical oxidation process is the applied potential. It determines which reactions will occur within the solution, and the electrolysis kinetics interferes with energy consumption and process cost.

Fig. 8b shows the effect of voltage variation (5–15 V) on the discoloration of the MB containing 0.1 mol L^{-1} Na_2SO_4 and 20 mmol L^{-1} NaCl solution. As for the NaCl concentration, there is an optimal voltage value. At 5 V, there was incomplete discoloration; at 10 and 15 V, total discoloration occurs within 60 min of electrolysis. Thus, increasing the potential from 5 to 10 V favored the removal of color; however, applying 15 V shows a lower rate of discoloration. This behavior shows that, at 15 V, despite generating a greater amount of oxidizing species, these species are also consumed, favoring parallel reactions, such as oxygen evolution [41] and the oxidation of active chlorine into ClO_3^- and ClO_4^- [56] instead of dye oxidation reactions.

TOC removal behavior (Table 3) is similar to color removal as a function of applied potential. Therefore, the use of 10 V promoted both faster discoloration and more significant TOC removal (64.0%). Data in Table 3 suggest that the current is mainly directed to the oxidation of the MB at the 5 V potential, and the increase in potential decreases the current efficiency due to the influence of parallel reactions. However, degradation performed at 5.0 V does not achieve full-color removal, and degradation at 15.0 V in addition to consuming more energy has low efficiency too. Thus, the most promising potential for removing color and TOC is 10.0 V, which has an energy consumption of 718.0 kWh kg^{-1}.

The pH of the solution is an essential factor in the electrochemical treatment of organic compounds, as it can determine the oxidizing species present in solution. There is still no consensus on the influence of pH on organic degradation efficiency. These divergences can result from the differences in the electrolytes, organic compounds, and electrode material [57-60]. However, in general, acid pH favors the degradation reaction because the hydroxyl radical presents higher oxidative capacity at lower pH according to the Nernst equation [61]. Also, the deactivation of

hydroxyl radicals leading to O_2 formation is disadvantaged at acid pH [51]. Therefore, it is necessary to evaluate the influence of pH on the degradation efficiency of organic compounds.

The pH of the electrolyte solutions was an essential factor for the electrochemical oxidation of MB using the Ti/$(RuO_2)_{0.5}(IrO_2)_{0.5}$ anode, especially in the TOC removal parameter (Fig. 8c). Three pH conditions were investigated, two pH-adjusted solutions - at alkaline medium (pH 10) or acidic (pH 2) and another condition with the initial solution without pH adjustment (pH 6). Note that the discoloration is favored at pH 10 or 2, and under all conditions, total color removal occurs. Conversely, at pH 6 there was a more significant removal of TOC (64.0%), and at pH 10 it was the lowest removal of TOC (20.0%). The low removal of TOC at pH 2 led to higher energy consumption (2869.2 kWh kg^{-1}) and lowered the current efficiency (3.1%). In NaCl medium, the variation in the initial pH affects the active species of the electrogenerated chlorine and its oxidation potential [63]. It is known that at pH < 3, the species chlorine (Cl_2) are predominant, while at pH 3–7.5, it is hypochlorous acid (HClO) and for pH > 7.5, the hypochlorous ion (ClO^-) and among these the HClO has the highest oxidation potential [64]. Then, Cl^- mediated oxidation of dyes with these species is expected to be faster in acidic than in alkaline medium [19, 20]. From this, the pH directly influences the efficiency of the process, thereby corroborating with the data found in this work, where tests conducted at pH 6 exhibit the best results.

In this work, the removal of TOC was favored at pH 6 followed by pH 10, leading to higher TOC removals, lower energy consumption, and higher mineralization current efficiency (Table 3). Saaidia et al. [60] also studied the efficiency of discoloration and removal of COD from MB solutions; they observed that increasing pH decreases the system efficiency (PbO_2 as the working electrode and stainless steel as the counter electrode, in Na_2SO_4 medium). The study also showed

that the current density, the temperature, the support electrolyte concentration, and the stirring speed influence the efficiency of both MB discoloration and mineralization.

The TOC removal was favored at pH 6. According to Martínez-Huitle et al. [63], the pH value can have several effects, as in the homogeneous decomposition of oxidants, as is the case of the reaction between hypochlorous acid and hypochlorite ($ClO + 2HClO \rightarrow ClO_3^- + 2Cl^- + 2H^+$), which can occur at its maximum rate in almost neutral pH, in the high loss of chlorine gas for pH <2 and in the oxidation capacity of organics, since acid-base equilibria can produce structures with different behaviors in degradation. Therefore, there is no need for an initial pH adjustment of the solution in the optimal degradation condition. Additionally, the final pH showed variation ± 0.5, when compared to the initial value. The direct comparison of these results is not an easy task due to the different experimental conditions tested. Table 4 summarizes the experimental conditions and the main results reported.

Table 4: Comparison of the performance of different anodes for the degradation of methylene blue.

Anode	Experimental conditions	Best results	Reference
$Ti/IrO_2–Ta_2O_5$	j = 40 mA cm^{-2}; C_0 = 100 mg L^{-1}; Electrolyte = 0.02 mmol L^{-1} Na_2SO_4 + 0.017 mmol L^{-1} NaCl; V = 1 L; Anode area = 63.5 cm^2; t = 360 min	Color removal = 100% COD removal = 86%	[25]
RuO_2/TiO_2 nanotube arrays	Lamp = 18 W; C_0 = 8 mg L^{-1}; Electrolyte = 15 g L^{-1} Na_2SO_4; V = 0.012 L; pH = 2; t = 120 min	Color removal = 65%	[44]
$Ti/TiRuO_2$	*j* = 20 mA cm^{-2}; C_0 = 80 mg L^{-1};	Color removal = 100% COD removal = 100%	[53]

	Electrolyte = 0.5 mol L^{-1} Na_2SO_4 +, 1.2 g of Cl^-; v = 0.5 L; Anode area = 50 cm^2; t = 150 min		
Ti/Pt	j= 50 mA cm^{-2}; C_0 = 60 mg L^{-1} Electrolyte= 0.5 mol L^{-1} H_2SO_4; V = 0.35 L; Anode area=15 cm^2 t = 460 min	Color removal = 100% COD removal= 80% TOC removal =75%	[64]
Ti/RuO_2–IrO_2	j = 40 mA cm^{-2}; C_0 = 100 mg L^{-1} Electrolyte = 0.1 mol L^{-1} NaCl; V = 0.1 L; Anode area = 1 cm^2; t = 90 min	Color removal =100% COD removal = 73%	[65]
La-doped RuO_2-TiO_2/Ti	j = 11 mA cm^{-2}; C_0 = 10 mg L^{-1}; Electrolyte = 0.1 mol L^{-1} Na_2SO_4; V = 0.1 L; Anode area = 1 cm^2 t=90 min	Color removal = 75%	[66]
Ti/Pt	j = 400 mA cm^{-2}; C_0 = 180 mg L^{-1}; V = 0.4 L; Anode area = 1 cm^2; t = 120 min	TOC removal = 93%	[67]
Boron-doped diamond	j = 30 mA cm^{-2}; C_0 = 100 mg L^{-1}; Electrolyte = 0.1 mol L^{-1} NaCl; V = 0.5 L; Anode area = 78 cm^2	COD removal = 100% TOC removal =100%	[68]
Ti/RuO_2–IrO_2	E = 10 V; C_0 = 50 mg L^{-1}; Electrolyte = 0.1 mol L^{-1} Na_2SO_4 + 20 mmol L^{-1} NaCl; V = 0.22 L; Anode area = 2 cm^2; t = 60 min	Color removal =100% COD removal = 64%	This Work

4. Conclusions

Ti/$(RuO_2)_{0.5}(IrO_2)_{0.5}$ anodes were successfully synthesized by using microwave and compared with the anodes obtained by the conventional method. Microwave irradiation leads to compact films for all calcination temperatures studied. The higher voltammetric charges found for the microwave-made anodes were attributed to smaller crystallite sizes (1.6 times) and the changes in the bonding environment caused by rapid heating. Furthermore, service life was extremely prolonged (increased

15 years) for anodes produced by microwave at 350 ºC, found as the most suitable temperature. Therefore, it was selected electrochemical degradation assays of the methylene blue dye degradation to evaluate its electrocatalytic properties. The electrocatalytic activity of the anode produced by microwaves was satisfactory, as removal of 64% of the TOC and 100% of the color were yielded in just one hour.

Finally, the Ti/$(RuO_2)_{0.5}(IrO_2)_{0.5}$ anode obtained by the hybrid heating method using microwave irradiation is a promisor anode material capable of being efficiently employed in dye degradation processes. Moreover, the high electrocatalytic activity, long service life, and lower resistivity when compared to those obtained by the conventional method, makes this material very attractive for industrial MMO production.

Acknowledgments

Financial support from the Agencia Estatal de Investigación through project CTM2016-76197-R (AEI/FEDER, UE) is gratefully acknowledged. This study was also financed by the Brazilian agencies Coordenação de Aperfeiçoamento de Pessoal de Nível Superior - CAPES (88882.365552/2018-01 and 88881.187890/2018-01), CNPq (305438/2018-2, 311856/2019-5 and 142034/2020-7) and FAPITEC/SE.

5. References

[1] Mattos-Costa, F. I.; de Lima-Neto, P.; Machado, S. A. S.; Avaca, L. A. Characterisation of Surfaces Modified by Sol-Gel Derived $Ru_xIr_{1-x}O_2$ Coatings for Oxygen Evolution in Acid Medium. *Electrochim. Acta* **1998**, *44*, 1515–1523. https://doi.org/10.1016/S0013-4686(98)00275-8.

[2] Fabbri, E.; Habereder, A.; Waltar, K.; Kötz, R.; Schmidt, T. J. Developments and Perspectives

of Oxide-Based Catalysts for the Oxygen Evolution Reaction. *Catal. Sci. Technol.* **2014**, *4*, 3800–3821. https://doi.org/10.1039/c4cy00669k.

[3] Gawande, M. B.; Pandey, R. K.; Jayaram, R. V. Role of Mixed Metal Oxides in Catalysis Science—versatile Applications in Organic Synthesis. *Catal. Sci. Technol.* **2012**, *2*, 1113. https://doi.org/10.1039/c2cy00490a.

[4] Trasatti, S. Electrocatalysis: Understanding the Success of DSA®. *Electrochim. Acta* **2000**, *45*, 2377–2385. https://doi.org/10.1016/S0013-4686(00)00338-8.

[5] Wang, G.; Zhang, L.; Zhang, J. A Review of Electrode Materials for Electrochemical Supercapacitors. *Chem. Soc. Rev.* **2012**, *41*, 797–828. https://doi.org/10.1039/c1cs15060j.

[6] Souza, F. L.; Aquino, M.; Miwa, D. W.; Rodrigo, M. A.; Motheo, A. J. Photo-Assisted Electrochemical Degradation of the Dimethyl Phthalate Ester on DSA®. Electrode. *J. Environ. Chem. Eng.* **2014**, *2*, 811–818. https://doi.org/10.1016/j.jece.2014.02.003.

[7] Santos, T. É S.; Silva, R. S.; Meneses, C. T.; Martínez-Huitle, C. A.; Eguiluz, K. I. B.; Salazar-Banda, G. R. Unexpected Enhancement of Electrocatalytic Nature of Ti/$(RuO_2)_x$-$(Sb_2O_5)_y$ Anodes Prepared by the Ionic Liquid-Thermal Decomposition Method. *Ind. Eng. Chem. Res.* **2016**, *55*, 3182–3187. https://doi.org/10.1021/acs.iecr.5b04690.

[8] de Mello, R.; Santos, L. H. E.; Pupo, M. M. S.; Eguiluz, K. I. B.; Salazar-Banda, G. R.; Motheo, A. J. Alachlor Removal Performance of Ti/$Ru_{0.3}Ti_{0.7}O_2$ Anodes Prepared from Ionic Liquid Solution. *J. Solid State Electrochem.* **2017**, 22, 1571-1580 https://doi.org/10.1007/s10008-017-3700-6.

[9] Jeng, J.-S. The Influence of Annealing Atmosphere on the Material Properties of Sol–gel Derived SnO_2:Sb Films before and after Annealing. *Appl. Surf. Sci.* **2012**, *258*, 5981–5986. https://doi.org/10.1016/j.apsusc.2012.02.010.

[10] Shao, D.; Li, X.; Xu, H.; Yan, W. A Simply Improved Ti/Sb-SnO_2 Electrode with Stable Adn High Performance in Electrochemical Oxidation Process. *RSC Adv.* **2014**, *4*, 21230–21237. https://doi.org/10.1039/C4RA01990C.

[11] Pechini, M. P.; Adams, N. Method of Preparing Lead and Alkaline Earth Titanates and Niobates and Coating Method Using the Same to Form a Capacitor. *United states patent office*. 1967, 01–07.

[12] Zhang, Q.; Liu, Y.; Zeng, D.; Lin, J.; Liu, W. The Effect of Ce Doped in Ti/SnO_2-Sb_2O_3/SnO_2-Sb_2O_3-CeO_2 Electrode and Its Electro-Catalytic Performance in Caprolactam Wastewater.

Water Sci. Technol. **2011**, *64*, 2023–2028. https://doi.org/10.2166/wst.2011.613.

[13] Mingos, D. M. P. Theoretical Aspects of Microwave Dielectric Heating. *Microw. Assist. Org. Synth.* **2009**, 1, 1–22. https://doi.org/10.1002/9781444305548.ch1.

[14] Aquino, J. M.; Rocha-Filho, R. C.; Bocchi, N.; Biaggio, S. R. Microwave-Assisted Crystallization into Anatase of Amorphous TiO_2 Nanotubes Electrochemically Grown on a Ti Substrate. *Mater. Lett.* **2014**, *126*, 52–54. https://doi.org/10.1016/j.matlet.2014.04.005.

[15] Basak, T.; Priya, A. S. Role of Ceramic Supports on Microwave Heating of Materials. *J. Appl. Phys.* **2005**, *97*, 1-28. https://doi.org/10.1063/1.1871356.

[16] Bilecka, I.; Niederberger, M. Microwave Chemistry for Inorganic Nanomaterials Synthesis. *Nanoscale* **2010**, *2*, 1358–1374. https://doi.org/10.1039/b9nr00377k.

[17] Gonzaga, I. M. D.; Andrade, A. C. A.; Silva, R. S.; Salazar-Banda, G. R.; Cavalcanti, E. B.; Eguiluz, K. I. B. Synthesis of high-area chemically modified electrodes using microwave heating. *Chem. Eng. Commun.* **2019**, *206*, 647–653. https://doi.org/10.1080/00986445.2018.1516645.

[18] Oghbaei, M.; Mirzaee, O. Microwave versus Conventional Sintering: A Review of Fundamentals, Advantages and Applications. *J. Alloys Compd.* **2010**, *494*, 175–189. https://doi.org/10.1016/j.jallcom.2010.01.068.

[19] Brillas, E., Martínez-Huitle, C. A. Decontamination of wastewaters containing synthetic organic dyes by electrochemical methods. An updated review. *Appl. Catal. B-Environ.* **2015**, 166, 603-643. https://doi.org/10.1016/j.apcatb.2014.11.016

[20] Moreira, F. C., Boaventura R. A. R., Brillas, E. Vilar, V. J. P. Electrochemical advanced oxidation processes: a review on their application to synthetic and real wastewaters. *Appl. Catal. B-Environ.* **2017**, 202, 217–261. https://doi.org/10.1016/j.apcatb.2016.08.037.

[21] Paz, A.; Carballo, J.; Pérez, M. J.; Domínguez, J. M. Biological Treatment of Model Dyes and Textile Wastewaters. *Chemospere*. **2017**, 181, 168–177. https://doi.org/10.1016/j.chemosphere.2017.04.046.

[22] Jiang, M.; Ye, K.; Deng, J.; Lin, J.; Ye, W.; Zhao, S.; Van Der Bruggen, B. Conventional Ultrafiltration As Effective Strategy for Dye/Salt Fractionation in Textile Wastewater Treatment. *Environ. Sci. Technol.* **2018**, *52*, 10698–10708. https://doi.org/10.1021/acs.est.8b02984.

[23] Ganiyu, S. O., Martínez-Huitle, C. A., Rodrigo, M. A. Renewable energies driven

electrochemical wastewater/soil decontamination technologies: A critical review of fundamental concepts and applications. *Appl. Catal. B-Environ.* **2020**, 270, 1–36. https://doi.org/10.1016/j.apcatb.2020.118857

[24] Lacasa, E., Cotillas, S., Saez, C., Lobato, J., Cañizares, P., Rodrigo, M. A. Environmental applications of electrochemical technology. What is needed to enable full-scale applications? *Curr. Opin. Electrochem.* **2019**, 16, 149–156.

[25] Pontes, J. P. S. D.; da Costa, P. R. F.; da Silva, D. R.; Garcia-Segura, S.; Martínez-Huitle, C. A. Methylene Blue Decolorization and Mineralization by Means of Electrochemical Technology at Pre-Pilot Plant Scale : Role of the Electrode Material and Oxidants. *Int. J. Electrochem. Sci.* **2016**, *11*, 4878–4891. https://doi.org/10.20964/2016.06.2.

[26] Rafatullah, M.; Sulaiman, O.; Hashim, R.; Ahmad, A. Adsorption of Methylene Blue on Low-Cost Adsorbents : A Review. *J. Hazard. Mater.* **2010**, *177*, 70–80. https://doi.org/10.1016/j.jhazmat.2009.12.047.

[27] Dória, A. R., Silva, R. S., Júnior, P. H. O., dos Santos, E. A., Mattedi, S., Hammer, P., Salazar-Banda G. R., Eguiluz, K. I. B. Influence of the RuO_2 layer thickness on the physical and electrochemical properties of anodes synthesized by the ionic liquid method. *Electrochim. Acta* **2020**, 136625, Pre-proof. https://doi.org/10.1016/j.electacta.2020.136625

[28] Da Silva, L. M.; De Faria, L. A.; Boodts, J. F. C. Determination of the Morphology Factor of Oxide Layers. *Electrochim. Acta* **2001**, *47*, 395–403. https://doi.org/10.1016/S0013-4686(01)00738-1.

[29] Wang, S.; Xu, H.; Yao, P.; Chen, X. Ti/RuO_2-IrO_2-SnO_2-Sb_2O_5 Anodes for Cl_2 Evolution from Seawater. *Electrochemistry* **2012**, *80*, 507–511.

[30] Martínez-Huitle, C. A.; Quiroz, M. A.; Comninellis, C.; Ferro, S.; De Battisti, A. Electrochemical Incineration of Chloranilic Acid Using Ti/IrO_2, Pb/PbO_2 and Si/BDD Electrodes. *Electrochim. Acta* **2004**, *50*, 949–956. https://doi.org/10.1016/j.electacta.2004.07.035.

[31] Santos, M. O.; Santos, G. O. S.; Mattedi, S.; Griza, S.; Eguiluz, K. I. B; Salazar-Banda, G. R. Influence of the Calcination Temperature and Ionic Liquid Used during Synthesis Procedure on the Physical and Electrochemical Properties of Ti/$(RuO_2)_{0.8}$–$(Sb_2O_4)_{0.2}$ Anodes. *J. Electroanal. Chem.* **2018**, *829*, 116–128. https://doi.org/10.1016/j.jelechem.2018.10.013.

[32] Santos, G. O. S.; Silva, L. R. A.; Alves, Y. G. S.; Silva, R. S.; Eguiluz, K. I. B.; Salazar-Banda,

G. R. Enhanced Stability and Electrocatalytic Properties of Ti/$Ru_xIr_{1-x}O_2$ Anodes Produced by a New Laser Process. *Chem. Eng. J.* **2019**, *355*, 439–447. https://doi.org/10.1016/j.cej.2018.08.145.

[33] Audichon, T.; Napporn, T. W.; Canaff, C.; Morais, C.; Comminges, C.; Kokoh, K. B. IrO_2 Coated on RuO_2 as Efficient and Stable Electroactive Nanocatalysts for Electrochemical Water Splitting. *J. Phys. Chem. C* **2016**, *120*, 2562–2573. https://doi.org/10.1021/acs.jpcc.5b11868.

[34] Morgan, D. J. Resolving Ruthenium : XPS Studies of Common Ruthenium Materials. *Surf. Interface Anal.* **2015**, 8, 1072–1079. https://doi.org/10.1002/sia.5852.

[35] Liu, B.; Wang, S.; Wang, C.; Chen, Y.; Ma, B. Surface Morphology and Electrochemical Properties of RuO_2 -Doped Ti/IrO_2-ZrO_2 Anodes for Oxygen Evolution Reaction. *J. Alloy. Compd.* **2019**, *778*, 593–602. https://doi.org/10.1016/j.jallcom.2018.11.191.

[36] Lemmon, E. W.; McLinden, M. O.; Friend, D. G. The NIST Chemistry WebBook, NIST Standard Reference Database; 2017. https://doi.org/10.18434/T4D303.

[37] Berenguer, R.; Sieben, J. M.; Quijada, C.; Morallón, E. Pt- and Ru-Doped SnO_2−Sb Anodes with High Stability in Alkaline Medium Rau L. *Appl. Mater. Interfaces* **2014**, *6*, 22778–22789.

[38] Muñoz-Moralez, M.; Braojos, M.; Sáez, C.; Cañizares, P.; Rodrigo, M. A. Remediation of Soils Polluted with Lindane Using Surfactant- Aided Soil Washing and Electrochemical Oxidation. *J. Hazard. Mater.* **2017**, *339*, 232–238. https://doi.org/10.1016/j.jhazmat.2017.06.021.

[39] Smith, R. D. L.; Sporinova, B.; Fagan, R. D.; Trudel, S.; Berlinguette, C. P. Facile Photochemical Preparation of Amorphous Iridium Oxide Films for Water Oxidation Catalysis. *Chem. Mater.* **2014**, 26, 1654-1659. https://doi.org/10.1021/cm4041715

[40] Shao, D.; Li, X.; Xu, H.; Yan, W. An Improved Stable Ti/Sb–SnO_2 Electrode with High Performance in Electrochemical Oxidation. *R. Soc. Chem.* **2014**, *4*, 21230–21237. https://doi.org/10.1039/c4ra01990c.

[41] Zaviska, F.; Drogui, P.; Blais, J. F.; Mercier, G. In Situ Active Chlorine Generation for the Treatment of Dye-Containing Effluents. *J. Appl. Electrochem.* **2009**, *39*, 2397–2408. https://doi.org/10.1007/s10800-009-9927-x.

[42] Audichon, T.; Benoit, A.; Steve, G.; Cretin, M.; Lamy, C.; Coutanceau, C. Preparation and Characterization of Supported $Ru_xIr_{(1-x)}O_2$ Nano-Oxides Using a Modified Polyol Synthesis Assisted by Microwave Activation for Energy Storage Applications. *Appl. Catal. B Environ.*

2016, *200*, 493–502. https://doi.org/10.1016/j.apcatb.2016.07.048.

[43] Audichon, T.; Morisset, S.; Napporn, T. W.; Kokoh, K. B.; Comminges, C.; Morais, C. Effect of Adding CeO_2 to RuO_2 -IrO_2 Mixed Nanocatalysts: Activity towards the Oxygen Evolution Reaction and Stability in Acidic Media. *ChemElectroChem* **2015**, *2*, 1128–1137. https://doi.org/10.1002/celc.201500072.

[44] Wang, Z., Liu, B., Xie, Z., Li, Y., Shen, Z. Y. Preparation and photocatalytic properties of RuO_2/TiO_2 composite nanotube arrays. *Ceram. Int.* **2016**, 42, 13664-13669. http://dx.doi.org/10.1016/j.ceramint.2016.05.164

[45] Bezerra, C. W. A. , Santos, G. O. S., Pupo, M. M. S., Gomes, M. A., da Silva, R. S., Eguiluz, K. I. B., Salazar-Banda, G. R. Novel eco-friendly method to prepare Ti/RuO_2–IrO_2 anodes by using polyvinyl alcohol as the solvent. *J. Electroanal. Chem.* **2020**, 859, 113822. https://doi.org/10.1016/j.jelechem.2020.113822

[46] Hoseinieh, S. M.; Ashrafizadeh, F. Influence of Electrolyte Composition on Deactivation Mechanism of a Ti/$Ru_{0.25}Ir_{0.25}Ti_{0.5}O_2$ Electrode. *Ionics.* **2013**, *19*, 113–125. https://doi.org/10.1007/s11581-012-0737-5.

[47] Zhang, J.; Hu, J.; Zhang, J.; Cao, C. IrO_2-SiO_2 Binary Oxide Films : Geometric or Kinetic Interpretation of the Improved Electrocatalytic Activity for the Oxygen Evolution Reaction. *Int. J. Hydrogen Energy* **2011**, *36*, 5218–5226. https://doi.org/10.1016/j.ijhydene.2011.01.131.

[48] Chaiyont, R.; Badoe, C.; de León, C. P.; Nava, J. L.; Recio, F. J.; Sirés, I.; Herrasti, P.; Walsh, F. C. Decolorization of Methyl Orange Dye at IrO_2-SnO_2-Sb_2O_5 Coated Titanium Anodes. *Chem. Eng. Technol.* **2013**, *36*, 123–129. https://doi.org/10.1002/ceat.201200231.

[49] Moradi, F.; Dehghanian, C. Addition of IrO_2 to RuO_2+TiO_2 coated Anodes and Its Effect on Electrochemical Performance of Anodes in Acid Media. *Prog. Nat. Sci. Mater. Int.* **2014**, *24*, 134–141. https://doi.org/10.1016/j.pnsc.2014.03.008.

[50] Comninellis, C. Electrocatalysis in the Electrochemical Conversion / Combustion of Organic Pollutants. *Electrochim. Acta* **1994**, *39*, 1857–1862. https://doi.org/10.1016/0013-4686(94)85175-1.

[51] Wu, W.; Huang, Z.-H.; Lim, T.-T. Recent Development of Mixed Metal Oxide Anodes for Electrochemical Oxidation of Organic Pollutants in Water. *Appl. Catal. A Gen.* **2014**, *480*, 58–78. https://doi.org/10.1016/j.apcata.2014.04.035.

[52] Panizza, M.; Michaud, P. A.; Cerisola, G.; Comninellis, C. H. Electrochemical Treatment of

Wastewaters Containing Organic Pollutants on Boron-Doped Diamond Electrodes: Prediction of Specific Energy Consumption and Required Electrode Area. *Electrochem. Commun.* **2001**, *3*, 336–339. https://doi.org/10.1016/S1388-2481(01)00166-7.

[53] Panizza, M.; Barbucci, A.; Ricotti, R.; Cerisola, G. Electrochemical Degradation of Methylene Blue. *Sep. Purif. Technol.* **2007**, *54*, 382–387. https://doi.org/10.1016/j.seppur.2006.10.010.

[54] Saxena, P.; Ruparelia, J. Influence of Supporting Electrolytes on Electrochemical Treatability of Reactive Black 5 Using Dimensionally Stable Anode. *J. Inst. Eng. Ser. A* **2019**, *100*, 299–310. https://doi.org/10.1007/s40030-019-00360-4.

[55] Liu, C.; Huang, C. P.; Hu, C.; Juang, Y.; Huang, C. Photoelectrochemical Degradation of Dye Wastewater on TiO_2-Coated Titanium Electrode Prepared by Electrophoretic *Sep. Purif. Technol.* **2016**, *165*, 153-165. https://doi.org/10.1016/j.seppur.2016.03.045.

[56] Panizza, M., Cerisola, G. Applicability of electrochemical methods to carwash wastewaters for reuse. Part 2: Electrocoagulation and anodic oxidation integrated process. *J. Electroanal. Chem.* **2010**, 638, 236-240. https://doi.org/10.1016/j.jelechem.2009.11.003

[57] Xu, L.; Guo, Z.; Du, L. Anodic Oxidation of Azo Dye C. I. Acid Red 73 by the Yttrium-Doped Ti/SnO_2-Sb Electrodes. *Front. Chem. Sci. Eng.* **2013**, *7*, 338–346. https://doi.org/10.1007/s11705-013-1335-4.

[58] Xu, L.; Guo, Z.; Du, L.; He, J. Decolourization and Degradation of C. I. Acid Red 73 by Anodic Oxidation and the Synergy Technology of Anodic Oxidation Coupling Nanofiltration. *Electrochim. Acta* **2013**, *97*, 150–159. https://doi.org/10.1016/j.electacta.2013.01.148.

[59] Zhou, M.; Särkkä, H.; Sillanpää, M. A Comparative Experimental Study on Methyl Orange Degradation by Electrochemical Oxidation on BDD and MMO Electrodes. *Sep. Purif. Technol.* **2011**, *78*, 290–297. https://doi.org/10.1016/j.seppur.2011.02.013.

[60] Saaidia, S.; Delimi, R.; Benredjem, Z.; Mehellou, A.; Djemel, A.; Barbari, K. Use of a PbO_2 electrode of a Lead-Acid Battery for the Electrochemical Degradation of Methylene Blue. *Sep. Sci. Technol.* **2017**, *52*, 1602–1614. https://doi.org/10.1080/01496395.2017.1291681.

[61] Vasconcelos, V. M.; De Souza, F. L.; Guaraldo, T. T.; Migliorini, F. L.; Baldan, M. R.; Ferreira, N. G.; De Lanza, M. R. V. Oxidação Eletroquímica Dos Corantes Reativos Preto 5 E Azul 19 Utilizando Um Eletrodo de Diamante Dopado Com Boro Não Comercial. *Quim. Nova* **2016**, *39*, 1051–1058. https://doi.org/10.5935/0100-4042.20160117.

[62] Wang, B.; Kong, W.; Ma, H. Electrochemical Treatment of Paper Mill Wastewater Using

Three-Dimensional Electrodes with Ti/Co/SnO_2-Sb_2O_5 Anode. *J. Hazard. Mater*. **2007**, *146*, 295–301. https://doi.org/10.1016/j.jhazmat.2006.12.031.

[63] Martínez-Huitle, C. A., Rodrigo, M. A., Sires, I., Scialdone, O. Single and coupled electrochemical processes and reactors for the abatement of organic water pollutants: a critical review. *Chem. Rev.* **2015**, 115, 13362-13407. https://doi.org/10.1021/acs.chemrev.5b00361

[64] Oliveira, G. R., Fernandes, N. S., de Melo, J. V., da Silva, D. R., Urgeghe, C., Martínez-Huitle, C. A. Electrocatalytic properties of Ti-supported Pt for decolorizing and removing dye from synthetic textile wastewaters. *Chem. Eng. J.* **2011**, 168, 208-214. https://doi.org/10.1016/j.cej.2010.12.070

[65] Baddouh, A., El Ibrahimi, B., Rguitti, M. M., Mohamed, E., Hussain, S., Bazzi, L. Electrochemical removal of methylene bleu dye in aqueous solution using Ti/RuO_2–IrO_2 and SnO_2 electrodes. *Sep. Sci. Technol*. **2020**, 55, 1852-1861. https://doi.org/10.1080/01496395.2019.1608244

[66] Zuo, J., Zhu, J., Zhang, M., Hong, Q., Han, J., Liu, J. Synergistic photoelectrochemical performance of La-doped RuO_2-TiO_2/Ti electrodes. *Appl. Surf. Sci.* **2020**, 502, 144288-144293. https://doi.org/10.1016/j.apsusc.2019.144288

[67] Yuan, S., Li, Z., Wang, Y. Effective degradation of methylene blue by a novel electrochemically driven process. *Electrochem. Commun.* **2013,** 29, 48-51. http://dx.doi.org/10.1016/j.elecom.2013.01.012

[68] Canizares, P., Louhichi, B., Gadri, A., Nasr, B., Paz, R., Rodrigo, M. A., Saez, C.. Electrochemical treatment of the pollutants generated in an ink-manufacturing process. *J. Hazard. Mat.* **2007**, 146, 552-557. http://dx.doi.org/10.1016/j.jhazmat.2007.04.085